Assessing the Robustness of a UAS Detect & Avoid Algorithm

Cyril Allignol, Nicolas Barnier, Nicolas Durand, Guido Manfredi, Éric Blond

Twelfth USA/Europe Air Traffic Management Research and Development Seminar (ATM2017)

Assessing the Robustness of a UAS Detect & Avoid Algorithm

Cyril Allignol, Nicolas Barnier, Nicolas Durand, Guido Manfredi
ENAC
7 av. Édouard Belin
31 055 Toulouse, France
firstname.lastname@enac.fr

Éric Blond
DSNA/DTI
1 av. du Dr Maurice Grynfogel
31 035 Toulouse, France
eric.blond@aviation-civile.gouv.fr

***Abstract*—In this article, we evaluate the robustness of a detect and avoid algorithm designed for the integration of UASs in terminal control areas. This assessment relies on a realistic modeling of navigation accuracy on positions and velocities and was carried out on thousands of scenarios built from recorded commercial traffic trajectories. The tested scenarios involved two different types of UASs – flying at 80 kts and 160 kts – with various missions, and three strategies for separation: one focussing on the separation distance, one focussing on the UAS mission and and combination of both.**

Fast-time simulation was used to evaluate each scenario against a wide range of accuracy levels corresponding to required navigation precision standards and linked to on-board navigation and communication systems. Experiments reveal a strong robustness of the separation algorithm up to relatively high uncertainty levels, indicating that UASs equipped with low accuracy navigation systems can still manage proper separation. However, the maneuvering cost for separation increases when the accuracy deteriorates. Nevertheless, a UAS with GPS-based navigation in a collaborative environment (e.g. aircraft providing their navigation parameters through ADS-B) can expect robustness at a reasonable cost.

***Keywords*—UAS, detect & avoid, robustness, navigation accuracy, self-separation, geometrical algorithm**

I. Introduction

Operations of unmanned aircraft systems (UASs) have drastically increased [1] in the past few years, as the technology has spread from military use to various civilian applications such as aerial surveying, search and rescue or scientific research. Due to the nature of these tasks, most UASs operate in the lower airspace, where their mission might interfere with airliners departures and arrivals at airports. The integration of UASs in terminal control areas (TCAs) has thus become a challenging problem both in ATM and on-board systems communities, so that research and development of systems and algorithms to ensure the separation between a UAS and regular traffic are on the rise.

Several strategies can be explored in this context. First, separation can be entirely managed by Air Navigation Service Providers. Experiments [2] showed that Air Traffic Controllers resolution process is hindered by UASs mixed with conventional traffic because they have unusual performance specifications and interact with different time responses.

Separation could otherwise be delegated to *both* commercial aircraft and UASs which could autonomously maneuver to resolve potential conflicts. However, complex processes of coordination should be considered in such a context to keep Air Traffic Controllers aware of the resolution process and able to interfere in it.

Finally, conflict resolution could be taken care of by UASs only such that they do not disrupt the commercial traffic. This seems a more realistic approach, provided that the positions and speeds of surrounding aircraft are available (through ADS-B for example) and that the performances of UASs and the resolution anticipation are sufficient to solve all traffic situations. In previous work [3], [4], [5], we investigated the latter strategy by adapting a self-separation algorithm used in robotics [6] to our context and carried out experiment with various parameters and strategies on real traffic samples. In this paper, we propose to test the robustness of this algorithm in presence of navigation errors by conducting a sensitivity analysis based on a probabilistic model of position and velocity accuracy.

A. Related Works

When the concept of Free-flight emerged in the 90s, one of the ideas was then to equip every aircraft with a detect and avoid algorithm able to ensure separation with the rest of the traffic.

The first effective approach used sliding forces to coordinate maneuvers between aircraft [7]. Potential or vortex fields [8] as well as a model based on an analogy with electrical particle repulsion [9] were also used. In 2001, we proposed a token allocation strategy combined with an A^* algorithm to solve conflicts with realistic maneuvers [10], [11]. Even if some maneuvers could be simultaneously decided, a complete ranking of aircraft was necessary and finding an optimal ranking has been shown to be problem-dependent [12]. We also tried artificial Neural Networks on the two-aircraft problem [13] but they could not be generalized to handle more aircraft. All these approaches have been tested on en-route traffic, mainly with leveled aircraft.

Geometrical algorithms have also been widely studied in robotics [14], [15], [16], [6]. The powerful Optimal Reciprocal Collision Avoidance (ORCA) technique developed by Van den

Berg et al. [6] can handle thousands of agents in a small space. It was applied to aircraft by Snape et al. [16], but the hypotheses of the algorithm require simultaneous vertical and horizontal speed changes. We also tested them [3] in the horizontal plane with speed constraints and showed that this algorithm is unable to deal with high densities of traffic when the speed norm cannot be changed.

More generally, conflict resolution has been proven to be a highly combinatorial optimization problem [17]. Most centralized approaches that have been proposed to solve conflicts can be broadly divided into two main categories. The first ones [18], [19], [20] use greedy sequential algorithms to optimize trajectories one after the other based on a ranking of aircraft (ordering aircraft is however very challenging [12]). The others try to find the global optimum without the need to prioritize aircraft. Among this second category, many models define aircraft trajectories through simple analytic expressions that introduce strong limits on the type of situations that can be dealt with, as the ones described in [21], [22], [23], [24], [25], [26]. In [27], [28], we proposed a model to solve multiple aircraft conflicts based on Metaheuristics (Genetic Algorithm and Tabu Search) using trajectory simulation with uncertainties. However, these works mainly targeted en-route traffic control and used simulated traffic only with the BADA model on real flight plans.

B. Detect & Avoid

In this article, we come back to a simpler problem in a more realistic environment. We consider UASs flying in the lower airspace (under FL180) and design various conflict scenarios with real recorded commercial aircraft trajectories in TCAs. The aim of the study is to assess the robustness of a "detect and avoid" strategy for UASs to maintain a reasonable horizontal separation with commercial traffic. The evaluated algorithm is derived from ORCA and was tested with different speed constraint hypotheses by Durand et al. [3] in the context of autonomous air conflict resolution. Compared to these first experiments, we then tailored this geometrical approach further in [4] and [5] to model the performances of UASs and consider specific fallback strategies to handle cases for which the first approach fails to maintain separation. The adaptation of ORCA to the integration of UASs in commercial traffic lead to the following major differences from the preliminary work:

- The whole avoidance maneuver is endorsed by the UAS.
- UASs used in a civilian context generally fly with low speeds compared to commercial aircraft. The ratio we used in this article can go from 1.5 to 5. We focus on the lower airspace where the aircraft speed is theoretically limited at $250\,\mathrm{kts}$, but recorded data show that in practice some aircraft fly much faster (up to $400\,\mathrm{kts}$). In this study, we consider two types of UASs: fast UASs flying at $160\,\mathrm{kts}$ and slow UASs flying at $80\,\mathrm{kts}$.
- Moreover, most civilian UASs have very poor speed up performances compared to conventional aircraft. We will therefore only consider maneuvers at constant speed for UASs, as this degree of freedom would have almost no effect on the resolution process with realistic traffic.
- Commercial aircraft flying in the lower airspace are generally climbing or descending and their speeds are constantly changing, either increasing when climbing, or decreasing when descending and changing direction as well. This factor has a great influence on the detect and avoid strategy in order to ensure that a reasonable distance to the encountered traffic can be maintained. Using real traffic data is therefore essential to validate a resolution algorithm for such evolving and intricate traffic.
- Air traffic trajectory prediction, which is one of the main component of a conflict solver, is always tainted with uncertainties that must be taken into account to assess the efficiency of an algorithm. We show how our approach can handle uncertainties by providing robust resolution maneuvers.

The main contribution in this paper is to perform a sensitivity analysis of such a solution, taking as input a realistic modeling of positioning and navigation sensors as the geometric algorithm is based on relative positions and speeds only.

C. Outline

Section II presents the geometrical algorithm and describes different strategies to choose the maneuver when a potential loss of separation is detected. In section III, we describe a probabilistic model for position and velocity accuracy that takes into account the time-correlation of successive measurement errors observed for many navigation sensors. This section also provides reference values for the uncertainty levels issued from reference documents. Section IV describes the simulation framework, scenarios and data used throughout our sensitivity analysis and shows the results obtained from almost $300\,000$ fast-time simulations. The impact of navigation errors on both the separation and the cost of maneuvers are analysed. The last section draws some conclusion on the robustness of our geometrical algorithm and highlights directions for future work.

II. Detect and Avoid Model

This section describes the Optimal Reciprocal Collision Avoidance (ORCA) algorithm developed in [6] and its adaptation to the case where only one aircraft (the UAS) maneuvers. We first detail how the constraints are computed for a single aircraft, then propose different strategies to modify the heading of the UAS in order to avoid the constraints with a fixed velocity. We also describe a fallback strategy to minimize the separation violation when our model has no solution within the allowed turning range. Our model is then further extended to simultaneously take into account several aircraft while keeping the UAS speed constant.

A. Constraint Model

Let d be the target separation distance and τ be a look ahead time. In figure 1, let us consider UAS A and aircraft B. We can represent the position of aircraft B in the referential of UAS A. If we draw a circle of radius d centered at aircraft B,

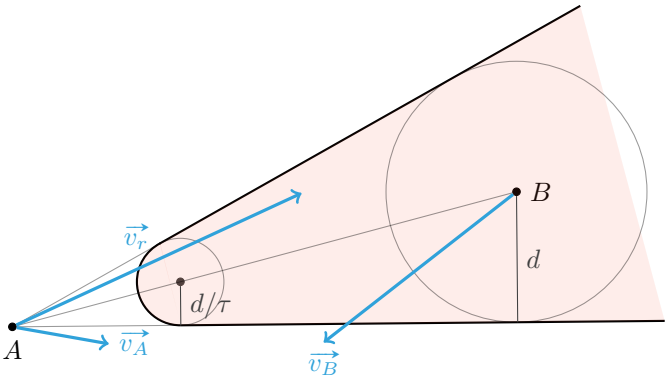

Figure 1. Conflicting aircraft model: a conflict will occur within time τ if and only if the relative speed $\overrightarrow{v_r}$ lies in the forbidden zone in red.

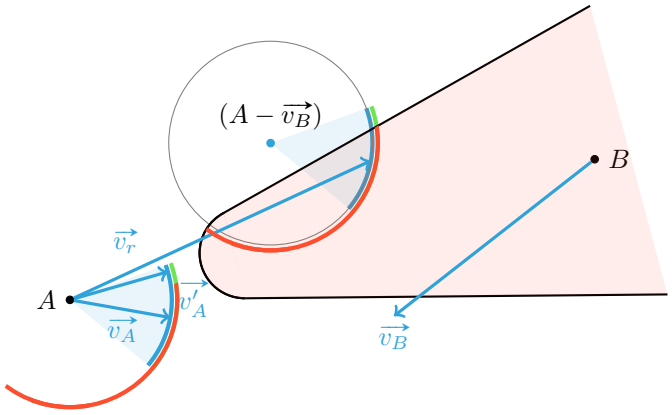

Figure 2. Possible headings for conflict avoidance: the end of $\overrightarrow{v'_r}$ must lie on the circle but outside of the forbidden zone (in light red) and in the allowed turn angle range of $\pm\theta$ ($\theta = 30°$) around $\overrightarrow{v_A}$, which leaves the tiny green safe zone as possible new heading for the UAS.

the two lines issued from position A, tangent to the circle of radius d form a cone. If the relative speed $\overrightarrow{v_r} = \overrightarrow{v_A} - \overrightarrow{v_B}$ lies in this cone, a conflict will occur in the future. If we draw a circle of size $\frac{d}{\tau}$ tangent to the two previous lines, we obtain a new zone (in light red) bounded by the bold line in figure 1. It is then straightforward to understand that a conflict will occur within time τ if and only if $\overrightarrow{v_r}$ lies in this zone. If this is the case, then it is necessary to modify the speed vector $\overrightarrow{v_A}$ in such a way that the resulting relative speed vector $\overrightarrow{v'_r}$ is outside of the constraint.

B. Possible Heading Range

In this paper, we consider that heading changes are the only possible maneuvers for UAS. Velocity changes were also considered, but were ruled out for several reasons:

- The capacity of a small UAS to accelerate is poor, so that a velocity increase would be limited in amplitude and would take too long to enforce.
- It has been observed in a previous study [5] that the higher the velocity of the UAS, the better the chances the avoiding maneuver has to succeed. Velocity reduction therefore seems unpromising.
- The velocity of UASs is low compared to aircraft. A slight modification of this velocity would be almost negligible.

To ensure that the norm of the speed of the UAS remains constant throughout the conflict resolution process, we must have:

$$\left\|\overrightarrow{v'_A}\right\| = \|\overrightarrow{v_A}\|$$

As $\overrightarrow{v'_r} = \overrightarrow{v'_A} - \overrightarrow{v_B}$, we also have:

$$(x_{v'_r} + x_{v_B})^2 + (y_{v'_r} + y_{v_B})^2 = \|\overrightarrow{v_A}\|^2$$

which means that the possible endpoints of $\overrightarrow{v'_r}$ belongs to a circle of radius $\|\overrightarrow{v_A}\|$ centered at $A - \overrightarrow{v_B}$ as shown on figure 2. But $\overrightarrow{v'_r}$ must also lie outside the forbidden zone defined in the previous section, which removes all angle ranges of the circle included in it (in red on the figure). The remaining angles must be further filtered by intersecting the allowed turn angle range θ corresponding to the performance of the UAS, i.e. an arc of $\pm\theta$ around the current speed shown in blue on figure 2 ($\theta = 30°$ in this paper).

The conflict-free heading change thus ranges over an arc of a circle (pictured in green on figure 2) which is the difference of the allowed (in blue) and forbidden (in red) arcs. In scenarios involving several conflicting aircraft, constraints are computed as described above for each aircraft, and the resulting constraint is simply the union of forbidden headings for each constraint, possibly containing several disjointed forbidden ranges.

C. Heading Change Strategies

As mentioned in the previous section, the conflict-free solution set is generally not a singleton, so a decision must be taken to choose the "best" angle within possibly discontinuous angle ranges. We define several possible strategies in the following sections.

1) Closest: The new speed for the UAS can be chosen with the available angle that minimizes the heading change, which will result in optimizing "maneuver quantity" (a measure defined in section IV-B). This strategy will be referred to as *Closest* in the remaining sections and is pictured in figure 3.

Because it is expected that the relative performance of airliners and UASs will create many unsolvable scenarios, for which losses of separation will occur, it likely preferable to choose an angle that leaves some leeway for the next resolution steps, i.e. which does not saturate the separation constraint.

2) Safest: To maximize the expectation of escaping a future conflict in case of further maneuvering of aircraft B (without any knowledge of its intended trajectory), the new heading could instead target the median value of the largest unconstrained angle range that at least intersects the maneuvering capacity of the UAS (in case of several disjointed angle ranges), which will optimize the robustness of the maneuver. This target heading is depicted in figure 3 as speed vector $\overrightarrow{v_{target}}$. Then the selected heading is simply the nearest

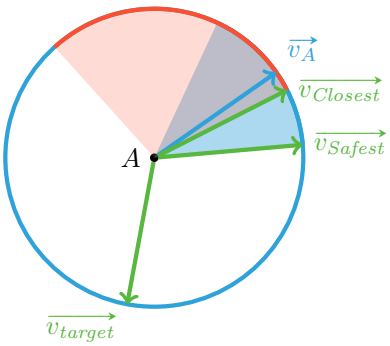

Figure 3. *Closest* and *Safest* speeds, computed from $\overrightarrow{v_A}$, given the constraints in red and turn angle range in blue.

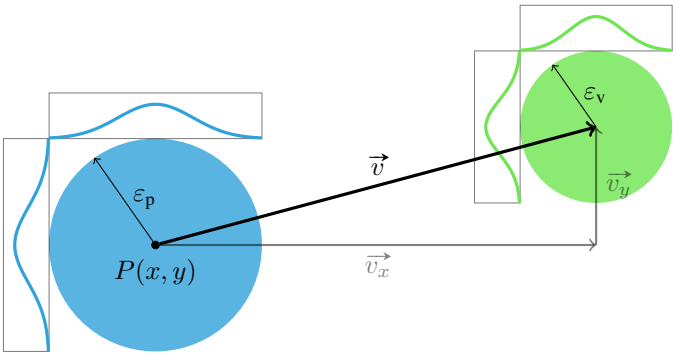

Figure 4. Modeling of accuracy: ε_p (resp. ε_v) represents the 95% accuracy bound for the position (resp. velocity) of UAS and aircraft. Each component of the position (resp.velocity) follows a normal distribution.

to this target in the maneuverability range. This strategy will be referred to as *Safest* below and its result is shown in figure 3.

However, the overestimate of the conflicting situation inherent to the *Safest* strategy can lead to unacceptable amounts of heading changes and totally disregards the UAS mission and flight plan.

3) Hybrid: The two strategies can in fact be combined to benefit from their respective advantages while getting rid of their drawbacks. The *Closest* strategy could be favored while there is still time and space to solve potential future conflicts, resorting to the *Safest* one before the situation becomes dire. So we define the *Hybrid* strategy parametrized by $\gamma \in \mathbb{R}^+$ for a set of (conflicting) aircraft positions $\mathcal{F}$ at a given time step:

$$Hybrid = \begin{cases} Closest & \text{if } \min_{B\in\mathcal{F}} \left\|\overrightarrow{AB}\right\| > \gamma d \\ Safest & \text{otherwise} \end{cases}$$

Therefore, this parameter allows us to continuously slide from a pure *Closest* strategy for $\gamma = 0$ to a pure *Safest* strategy for $\gamma = +\infty$; its influence on the detect and avoid algorithm was discussed in [5]. For our sensitivity analysis, we will consider strategies *Closest*, *Safest* and *Hybrid* with $\gamma = 3$.

4) Fallback Strategy: If the permitted heading range is empty, it means that no turning angle can guarantee the separation distance d for the next τ minutes. However, even if a conflict occurs, a brief one at a distance just below the target separation distance is preferable to a lasting close encounter.

To take into account this criterion while choosing a maneuver whenever a loss of separation is inevitable, our algorithm resorts to a fallback strategy consisting in reducing the separation distance until a solution can be found anew. Our current implementation uses a linear scheme with a constant step ($0.1\,\mathrm{NM}$ in our experiments) and returns the corresponding maneuver as soon as a solution is found.

III. Modeling Position and Velocity Errors

The efficiency of the detect and avoid algorithm described in the previous sections relies on the accuracy of UAS and aircraft positions and velocities gathered through ADS-B. This section presents a realistic model for uncertainties that will be used to assess the robustness of our algorithm.

A. Accuracy Categories

In order to comply with different airspace and procedure categories, the Radio Technical Commission for Aeronautics (RTCA) defines minimum system performance standards [29] that aircraft must meet in order to be allowed to enter a given type of airspace. Navigation Accuracy Categories for position (NACp) are defined as the $95\,\%$ accuracy metric that must be provided by the position source. These categories depend highly on the on-board equipment, and their values and associated accuracies are provided in table I. In the same manner, such categories are defined for velocity error (NACv, see table II).

As an example, the accuracy study for GPS from [30] indicates that a GPS-based aircraft can be categorized as NACp 9 and NACv 1 or 2, whereas [31] indicates that a satellite-based navigation system enhanced by ground stations (e.g. EGNOS[1], WAAS[2]) yields a NACp 10 accuracy level. This study proposes to assess the impact of accuracy category on the efficiency of our detect and avoid algorithm. The next section describes the modeling of position and velocity errors used for this sensitivity analysis.

B. Accuracy Model

The accuracy of navigation systems is, most of the time, expressed as a p-bound on the measurement error, where p is given as a percentage. Therefore, each measurement error could be represented as a normally distributed random variable.

In particular, we define ε_p as the $95\,\%$ accuracy bound on position, which ensures that $95\,\%$ of measures for position lie within a circle of radius ε_p centered on the actual aircraft (or UAS) position. In the same manner, we define ε_v as the $95\,\%$ accuracy bound on velocity. Each component of position and velocity (x, y, v_x, v_y) follows a normal distribution centered on the actual value of the estimated parameter. Figure 4 illustrates this uncertainty model.

However, this first model can produce consecutive values that would be arbitrarily distant from each other, whereas most measurement systems have an error that is time-correlated,

[1]European Geostationary Navigation Overlay Service
[2]Wide Area Augmentation System

Table I
NAVIGATION ACCURACY CATEGORIES FOR POSITION (NACP).

Category	NACp 1	NACp 2	NACp 3	NACp 4	NACp 5	NACp 6	NACp 7	NACp 8	NACp 9	NACp 10	NACp 11
Accuracy	10 NM	4 NM	2 NM	1 NM	0.5 NM	0.3 NM	0.1 NM	0.05 NM	30 m	10 m	3 m

Table II
NAVIGATION ACCURACY CATEGORIES FOR VELOCITY (NACV).

Category	NACv 1	NACv 2	NACv 3	NACv 4
Accuracy	$10\,\mathrm{m\,s^{-1}}$	$3\,\mathrm{m\,s^{-1}}$	$1\,\mathrm{m\,s^{-1}}$	$0.3\,\mathrm{m\,s^{-1}}$

i.e. the error on a given measure depends on the errors on the previous ones. Therefore, we decided to use the ADS-B accuracy model from [32], which proposes a similar probabilistic approach, except that it includes a correlation of errors on positions and speed over time. This model is briefly presented below.

We describe here how the time-correlated errors for each value are expressed. Let $X_1, X_2, \ldots, X_n$ be random variables such that X_i represents the error at time i (either on position (x or y) or velocity (v_x or v_y)) in our model, and r the target accuracy level (i.e. $r = \varepsilon_\mathrm{p}$ for position error model and $r = \varepsilon_\mathrm{v}$ for velocity error model). Then the sequence of variables X_i is modeled as a Markov chain described as:

$$X_i = e^{\frac{-1}{T}} X_{i-1} + U_i \tag{1}$$

where T is the time correlation of the process (T = 4 minutes in our study) and U_i is a random variable following a normal distribution[3] $\mathcal{N}(0, \sigma_u^2)$. The initial error (i.e. random variable X_0) follows a normal distribution $\mathcal{N}(0, \sigma_{X_0}^2)$.

The standard deviation for random variables X is deduced from the radial error on position (resp. velocity) and is computed according to the following equation:

$$\sigma_{X_0} = \frac{r}{\sqrt{-2\ln(1-p)}} \tag{2}$$

with $p = 95\,\%$ for our study. The variance of random variable U is deduced from the Markov process from equation 1 and the variance of X_0 from equation 2 as:

$$\sigma_u^2 = \sigma_{X_0}^2 (1 - e^{\frac{-2}{T}}) \tag{3}$$

Figure 5 shows the difference in the evolution of an uncorrelated normal distribution and a time-correlated distribution built according to the previously described scheme. Refer to [32] for complete details about this model.

The next section presents the results of a sensitivity analysis of the detect and avoid algorithm introduced in section II towards the accuracy model previously described.

IV. SENSITIVITY ANALYSIS

Our geometrical algorithm and accuracy model were implemented and used to perform a sensitivity analysis on a wide range of situations derived from real recorded TCA traffic.

[3]We note $\mathcal{N}(\mu, \sigma^2)$ a normal distribution with mean μ and variance σ^2.

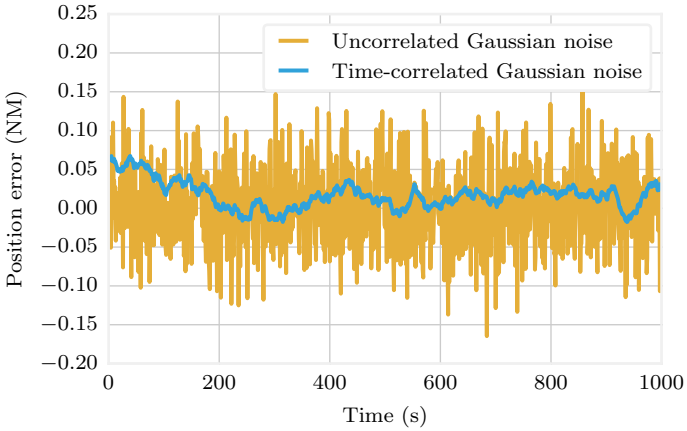

Figure 5. Comparison of an uncorrelated error (orange) and a time-correlated (T = 4 minutes) error on position for NACp 7 ($\varepsilon_\mathrm{p} = 0.1\,\mathrm{NM}$).

Section IV-A describes the data set and scenarios used in this study and section IV-B presents the results and analysis of our experiments.

A. Input Data and Scenarios

Experiments were conducted on real traffic data, recorded on 14th September 2013 in the TCA of Bordeaux in the south-west of France. This provides a particularly realistic picture of the types of trajectories that a UAS may encounter when flying in real traffic. This is all the more necessary because UASs are essentially meant to fly in the lower airspace where most commercial traffic is climbing or descending.

UAS trajectories are built from recorded tracks of aircraft with similar performances for two UAS types (flying at $80\,\mathrm{kts}$ and $160\,\mathrm{kts}$ respectively), three vertical profiles (leveled flight, climb and descent) and two horizontal profiles (constant heading and circle around a fixed point), for a total of 6 different patterns for each UAS type.

We filtered trajectories that had at least six minutes of flight under FL195, leaving us with a set of 475 aircraft trajectories. For each UAS type, six conflicting scenarios are built based on each aircraft trajectory by adequately inserting the UAS pre-computed trajectory in such a way that a collision would occur if no maneuver were issued. This procedure yields $6 \times 475 = 2850$ traffic situations for each aircraft type.

A fast-time simulator enables us to play the trajectories (both recorded and built) and to modify them by sending maneuver messages consisting of a heading change and a turn rate. Those messages are send to UASs only, other aircraft are left unchanged.

In our experiments, we aimed at a $3\,\mathrm{NM}$ separation between aircraft and UASs. We do not take vertical separation into

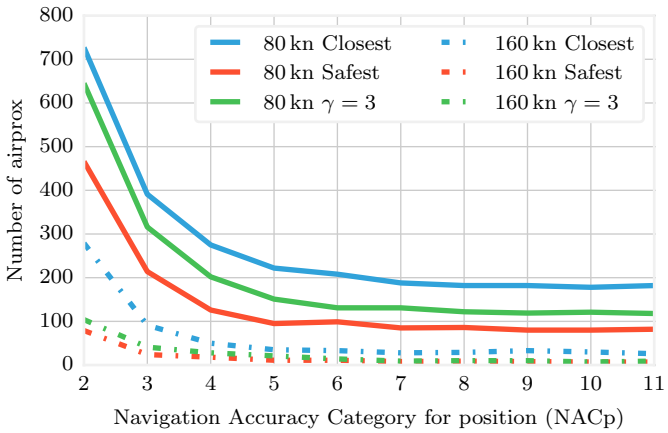

Figure 6. Evolution of the detect and avoid efficiency w.r.t. position accuracy. Velocity accuracy is fixed at NACv 2.

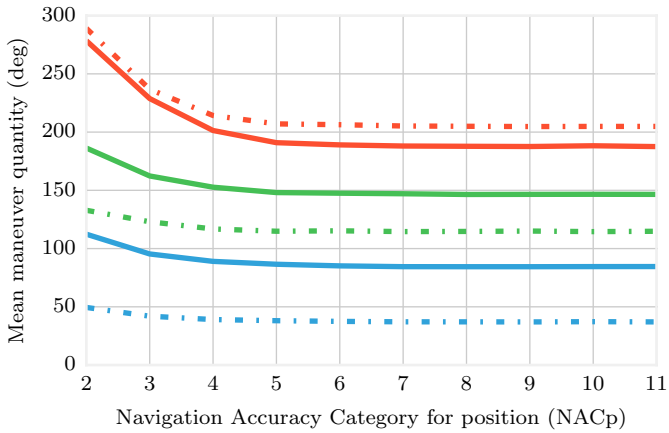

Figure 7. Evolution of the cost of conflict avoidance w.r.t. position accuracy. Velocity accuracy is fixed at NACv 2.

account because we want to test the efficiency of the detect and avoid process in the horizontal plane only. Further research will be conducted in the vertical dimension. The detect and avoid algorithm is triggered every ten seconds. The varying parameters in this sensitivity analysis are the navigation accuracy category for position and velocity, the UAS type (distinguished by their velocity) and the heading choice strategy (*Closest*, *Safest* or *Hybrid*). A total of 102 sets of parameters were tested, adding up to 290 700 fast-time simulations.

B. Influence of navigation accuracy on detect and avoid performance

For each set of parameters, all 2850 scenarios were run in a fast-time simulation tool (each run was executed within one tenth of a second on a 3.4 GHz Intel® Xeon® workstation). We measured various indicators of the efficiency of the conflict avoidance maneuvers and counted the occurrences of "close distance events," which we set up to be the simulations where the distance between the UAS and the aircraft went under 1 NM, and which we will call *airprox* in the following.

Figure 6 pictures the evolution of the number of such airproxes with position accuracy. The most interesting result is that there is a very low variation in the range NACp 6-11 (i.e. $\varepsilon_{\mathrm{p}} \leq 0.3\,\mathrm{NM}$), meaning that the detect and avoid algorithm is efficient even with reasonably high uncertainty about position (as stated in section III-A, a GPS-based UAS can be categorized NACp 8 or NACp 9). For lower accuracy categories however, the efficiency quickly deteriorates, particularly when the uncertainty ε_{p} is on the same order of magnitude as the target separation distance. With a higher UAS velocity (which is closely linked to its maneuverability, see [5]), the algorithm still shows high performance, as only 3 % to 4 % scenarios could not be solved for *Safest* and *Hybrid* strategies and a UAS flying at 160 kts.

The number of airprox events is the primary indicator for the efficiency of the detect and avoid strategy. Yet, the deviation of the UAS from its trajectory and the number of maneuvers matter as well: they can be seen as the cost of maintaining separation or as a secondary objective to discriminate between solutions with equivalent amounts of airprox. Let $(m_1, m_2, \ldots, m_k)$ be the sequence of heading maneuvers issued from the detect and avoid algorithm to the UAS for a given scenario. In order to quantify this cost of maneuvers, we define the *maneuver quantity* for this scenario as:

$$\mathrm{cost}(m_1, \ldots, m_k) = |m_1 - \mathrm{hdg}_0| + \sum_{i=2}^{k} |m_i - m_{i-1}|$$

where hdg_0 is the heading of the UAS before the first maneuver is issued.

Figure 7 shows the mean maneuver quantity for different position accuracy categories. For this criterion as well, the evolution is only significant for high error values ($\varepsilon_{\mathrm{p}} >= 1\,\mathrm{NM}$ or NACp 4 to 1). As observed in previous studies, the efficiency of conflict avoidance is increased at the cost of more deviation from the planned trajectory, with *Closest* strategy trying to limit this amount but sometimes failing the conflict resolution, *Safest* strategy giving priority to conflict avoidance no matter the cost of the maneuver, and *Hybrid* strategy combining both approaches. For the sake of readability, the legend for this figure and those which come after was not repeated and is the same as the legend for figure 6.

The same analysis has been carried out for velocity accuracy and the results can be seen on figures 8 and 9. Figure 8, which depicts the evolution of airprox events with respect to NACv, shows that our detect and avoid algorithm is very stable regarding speed uncertainties, as no increase in airprox events can be noticed. However, the impact on the cost of maneuvers, illustrated in figure 9, is significantly higher than for positioning error.

On the basis of observations from section III-A, we chose to plot the evolution of detect and avoid performance for several representative UAS configurations corresponding to different uncertainty levels. These configurations are described in table III, associated to their accuracy categories. As expected from the previous results, the number of airprox events

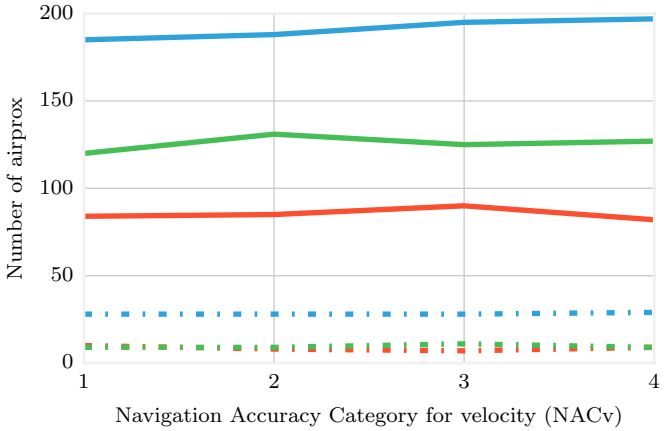

Figure 8. Evolution of the detect and avoid efficiency w.r.t. velocity accuracy. Position accuracy is fixed at NACp 7. The dotted red and dotted green plots overlap.

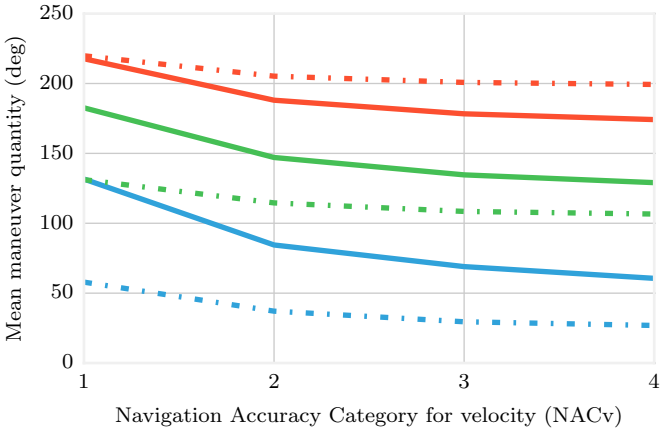

Figure 9. Evolution of the cost of conflict avoidance w.r.t. velocity accuracy. Position accuracy is fixed at NACp 7.

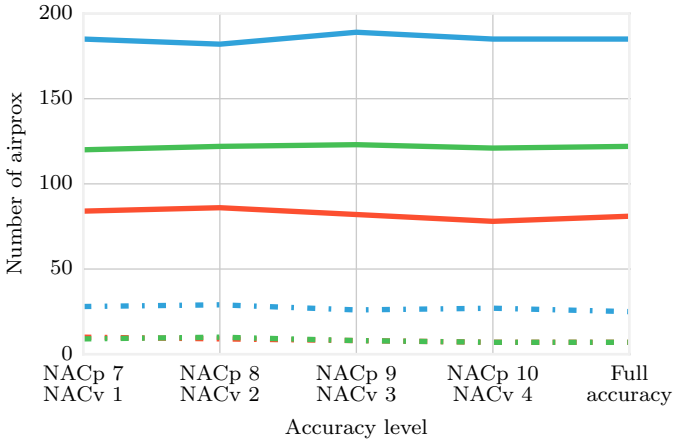

Figure 10. Evolution of the detect and avoid efficiency for various typical accuracy settings.

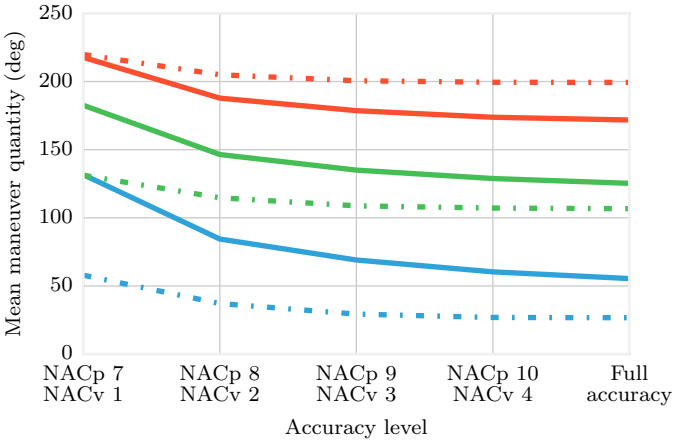

Figure 11. Evolution of the cost of conflict avoidance for various typical accuracy settings.

(figure 10) is stable. This means that our algorithm is robust as even a relatively inaccurate configuration (NACp 7 - NACv 1) can manage separation as well as a hypothetical fully accurate UAS. Figure 11, on the other hand, shows that a better equipped UAS will be able to maintain separation at a much lower cost, the most precise realistic configuration (NACp 10 - NACv 4) being very close to the best achievable maneuvers. A better assessment method for the cost of maneuvers would be to record the mission-time lost in the process of self-separation, which will be the subject of future work.

V. Conclusion and Future Work

Following previous work on a geometrical detect and avoid algorithm – derived from ORCA [6] – for the integration of unmanned aerial systems in terminal control areas, we proposed an analysis of the robustness of such an algorithm towards uncertainties on position and velocity measurements. Navigation errors have been modeled as random variables, taking into account the correlation of successive measurement errors over time that typically occurs in most sensors, and particularly in GPS receivers.

The sensitivity analysis was carried out on a set of 2850 realistic traffic scenarios issued from data recorded in a French TCA for two UAS models (flying at 80 kts and 160 kts respectively) and for three proposed resolution strategies: one that gives priority to separation (*Safest*) but leads to costly

Table III
Example UAS configurations and associated navigation accuracy categories.

	Accuracy categories	
Description	Position	Velocity
Hypothetical, fully accurate navigation	$\varepsilon_p = 0$	$\varepsilon_v = 0$
GPS-based navigation enhanced with ground stations (e.g. WAAS, EGNOS) combined with inertial navigation	NACp 10	NACv 4
Standard GPS-based navigation	NACp 9	NACv 3
GPS-based navigation with poor receiver antenna	NACp 8	NACv 2
Radar-based navigation	NACp 7	NACv 1

maneuvers, one that minimizes the amount of deviation from planned trajectory (*Closest*) at the cost of a slightly less efficient separation, and an intermediate strategy (*Hybrid*) that switches from the latter to the former whenever the separation distance falls below a given threshold. Many levels of position and velocity accuracy were tested, representing a wide range of UAS equipment for navigation and detection.

The most interesting result of this sensitivity analysis is the adequate robustness of the separation provided by our algorithm: only the most inaccurate configurations (e.g. with a positioning error greater than $0.5\,\mathrm{NM}$) significantly increase the number of airproxes in the simulations. Also, the velocity accuracy, at least for the categories defined by RTCA standards, has almost no influence on the capacity of the algorithm to ensure separation. However, lower accuracy levels induce an increase in the amount of deviation necessary to avoid the conflict.

In order to improve the accuracy of our model, other kinds of errors will be implemented in future developments. In particular, communication latency and errors of ADS-B transmitting systems can further deteriorate the accuracy of position and velocity measures. Furthermore, because ADS-B communications rely on antennas, masking effects can occur depending on the relative positions and angular state of aircraft and UASs, which can lead to missing data over short periods. Our detect and avoid algorithm already stores past positions and velocities for both the UAS and the adverse aircraft. This history would help recover from such situations by providing maneuvers based on previous states, but the impact on conflict avoidance has to be measured in future work.

In some TCAs, the UAS might face noncollaborative aircraft, i.e. aircraft that do not broadcast their position and speed through ADS-B (e.g. small private aircraft might not be equipped with ADS-B). In that case, the UAS shall rely on other sensors for the detection part, such as on-board radar, which are much less accurate. The analysis of such scenarios would require heterogeneous values for uncertainties, with high accuracy for UAS navigation and lower accuracy for aircraft position and velocity.

As pictured in our results, several traffic situations could not be efficiently solved, leading to an airprox. Because many aircraft are equipped with TCAS, it would be interesting to study how the detect and avoid algorithm and TCAS would behave when combined.

One of the pitfalls of our method is that it only takes into account the current positions and velocities, so that any further change in the aircraft state could break the resolution, especially with the *Closest* strategy. In order to improve the robustness of the maneuvers, we plan to try and anticipate better, both about aircraft intentions and UAS capabilities. Knowing the past positions of the aircraft, it is possible to build a short-term predicted trajectory based on the analysis of the derivatives of its speed and turn angle. For example, the beginning or the end of a turn, a climb or a descent could be inferred. Particular care would have to be taken during the calibration phase, especially when choosing the number of past states to consider: too many states would create some latency in predictions, whereas too few states would yield unreliable ones. If the aircraft trajectory could be predicted this way, then it would become particularly interesting to anticipate several maneuvers for the UAS. This could be planned optimally with an A* or Dijkstra algorithm, using the modified ORCA algorithm at each step to prune the search tree or validate the existence of partial solutions, at the cost of a significantly longer computation. It could also be performed geometrically by an approximation of a few maneuvers aggregated into a single one.

References

[1] ABIresearch, "Small unmanned aerial systems market exceeds US$8.4 billion by 2019, dominated by the commercial sector and driven by commercial applications," Jan. 2015. www.abiresearch.com/press/small-unmanned-arial-systems-market-exceeds-us84-b.

[2] Rockwell Collins France, Sagem, DSNA, and ENAC, "ODREA demonstration report," Tech. Rep. RPAS.06, SESAR Joint Undertaking, July 2015.

[3] N. Durand and N. Barnier, "Does ATM need centralized coordination? Autonomous conflict resolution analysis in a constrained speed environment," in *Proceedings of the 11th ATM R&D Seminar*, (Lisbon), June 2015.

[4] C. Allignol, N. Barnier, N. Durand, and E. Blond, "Detect & avoid, UAV integration in the lower airspace traffic," in *7th International Conference on Research in Air Transportation*, ICRAT 2016 Proceedings, (Philadelphia, PA), Drexel University, June 2016.

[5] C. Allignol, N. Barnier, N. Durand, G. Manfredi, and E. Blond, "Integration of UAS in terminal control area," in *35th Digital Avionics Systems Conference*, DASC 2016 Proceedings, (Sacramento, CA), IEEE/AIAA, Sept. 2016.

[6] J. van den Berg, S. J. Guy, M. Lin, and D. Manocha, "Reciprocal n-body collision avoidance," in *Robotics Research: The 14th International Symposium ISRR* (C. Pradalier, R. Siegwart, and G. Hirzinger, eds.), vol. 70 of *Springer Tracts in Advanced Robotics (STAR)*, (Berlin, Heidelberg), pp. 3–19, Springer, 2011.

[7] K. Zeghal, "A comparison of different approaches based on force fields for coordination among multiple mobiles," in *Proceedings. IEEE/RSJ International Conference on Intelligent Robots and Systems. Innovations in Theory, Practice and Applications*, vol. 1, pp. 273–278, Oct. 1998.

[8] J. Košecká, C. Tomlin, G. J. Pappas, and S. Sastry, "2 1/2 d conflict resolution maneuvers for atms," in *Proceedings of the 37th IEEE Conference on Decision and Control*, vol. 3, pp. 2650–2655, Dec. 1998.

[9] M. S. Eby and W. E. Kelly, III, "Free flight separation assurance using distributed algorithms," in *IEEE Aerospace Conference. Proceedings*, vol. 2, pp. 429–441, Mar. 1999.

[10] G. Granger, N. Durand, and J.-M. Alliot, "Token allocation strategy for free-flight conflict solving," in *IAAI 2001, 13th Conference on Innovative Applications of Artificial Intelligence* (H. Hirsh and S. Chien, eds.), (Seattle, WA), pp. 59–64, AAAI Press, Aug. 2001.

[11] G. Granger, N. Durand, and J.-M. Alliot, "Optimal resolution of en-route conflicts," in *Proceedings of the 4th ATM R&D Seminar*, (Santa Fe, NM), Dec. 2001.

[12] N. Archambault and N. Durand, "Scheduling heuristics for on-board sequential air conflict solving," in *23rd Digital Avionics Systems Conference*, vol. 1 of *DASC 2004 Proceedings*, (Salt Lake City, UT), pp. 3.1–9, AIAA, IEEE, Oct. 2004.

[13] N. Durand, J.-M. Alliot, and M. Frédéric, "Neural nets trained by genetic algorithms for collision avoidance," *Applied Intelligence*, vol. 13, pp. 205–213, Nov. 2000.

[14] I. Hwang, J. Kim, and C. Tomlin, "Protocol-based conflict resolution for air traffic control," *Air Traffic Control Quarterly*, vol. 15, no. 1, pp. 1–34, 2007.

[15] J. Le Ny and G. J. Pappas, "Geometric programming and mechanism design for air traffic conflict resolution," in *Proceedings of the 2010 American Control Conference (ACC)*, pp. 3069–3074, June 2010.

[16] J. Snape and D. Manocha, "Navigating multiple simple-airplanes in 3D workspace," in *IEEE International Conference on Robotics and Automation (ICRA)*, (Anchorage, AK), pp. 3974–3980, 2010.

[17] N. Durand, J.-M. Alliot, and J. Noailles, "Automatic aircraft conflict resolution using genetic algorithms," in *11th Annual Symposium on Applied Computing*, (Philadelphia, PA), pp. 289–298, ACM, Feb. 1996.
[18] F. Krella *et al.*, "Arc 2000 scenario (version 4.3)," tech. rep., Eurocontrol, Apr. 1989.
[19] Y.-J. Chiang, J. T. Klosowski, C. Lee, and J. S. Mitchell, "Geometric algorithms for conflict detection/resolution in air traffic management," in *Proceedings of the 36th Conference on Decision and Control*, vol. 2, (San Diego, CA), pp. 1835–1840, Dec. 1997.
[20] J. Hu, M. Prandini, A. Nilim, and S. Sastry, "Optimal coordinated maneuvers for three dimensional aircraft conflict resolution," *Journal of Guidance, Control and Dynamics*, vol. 25, pp. 888–900, Sept.–Oct. 2002.
[21] J.-H. Oh, J. M. Shewchun, and E. Feron, "Design and analysis of conflict resolution algorithms via positive semidefinite programming [aircraft conflict resolution]," in *Proceedings of the 36th Conference on Decision and Control*, vol. 5, (San Diego, CA), pp. 4179–4185, Dec. 1997.
[22] E. Frazzoli, Z.-H. Mao, J.-H. Oh, and E. Feron, "Resolution of conflicts involving many aircraft via semidefinite programming," *Journal of Guidance, Control and Dynamics*, vol. 24, pp. 79–86, Jan. 2001.
[23] L. Pallottino, A. Bicchi, and E. Feron, "Mixed integer programming for aircraft conflict resolution," in *AIAA Guidance, Navigation, and Control Conference and Exhibit*, (Montréal, Canada), Aug. 2001.
[24] L. Pallottino, E. Feron, and A. Bicchi, "Conflict resolution problems for air traffic management systems solved with mixed integer programming," *IEEE Transactions on Intelligent Transportation Systems*, vol. 3, pp. 3–11, Mar. 2002.
[25] M. A. Christodoulou and C. Kontogeorgou, "Collision avoidance in commercial aircraft free flight via neural networks and non-linear programming," *International Journal of Neural Systems*, vol. 18, pp. 371–387, Oct. 2008.
[26] M. Gariel and E. Feron, "3d conflict avoidance under uncertainties," in *28th Digital Avionics Systems Conference*, DASC 2009 Proceedings, (Orlando, FL), pp. 4.E.3–1–4.E.3–8, AIAA, IEEE, Oct. 2009.
[27] N. Durand and J.-M. Alliot, "Optimal resolution of en route conflicts," in *Proceedings of the 1st ATM R&D Seminar*, (Saclay, France), June 1997.
[28] C. Allignol, N. Barnier, N. Durand, and J.-M. Alliot, "A new framework for solving en-route conflicts," in *Proceedings of the 10th ATM R&D Seminar*, (Chicago, IL), June 2013.
[29] RTCA, Inc., Washington, DC, *Minimum Aviation System Performance Standards: Required Navigation Performance for Area Navigation*, June 2013. DO-236C.
[30] Department of Defense, *Global Positioning System – Standard Positioning Service – Performance Standard*, 4th ed., Sept. 2008.
[31] Department of Transportation – FAA, *Global Positioning System – Wide Area Augmentation System – Performance Standard*, 1st ed., Oct. 2008.
[32] S. C. Mohleji and G. Wang, "Modeling ADS-B position and velocity errors for airborne merging and spacing in interval management application," tech. rep., The MITRE Corporation, Sept. 2010.

AUTHORS

Cyril Allignol is an assistant professor at École Nationale de l'Aviation Civile (ENAC). He graduated from ENAC as an engineer in 2006, and received a Ph.D. (2011) in computer science from the University of Toulouse. His main research topics include combinatorial optimization, metaheuristics and their application to Air Traffic Management problems.

Nicolas Barnier is a lecturer and research assistant at ENAC. He graduated from ENAC as an engineer in 1997, and received a Ph.D. in computer science in 2002 from the University of Toulouse. He is one of the authors of FaCiLe, an open source Constraint Programming library for the functional language OCaml. His research interests focus on Constraint Programming, Local Search and Combinatorial Optimization in general.

Éric Blond graduated from ENAC as an engineer in 1975. He is currently (since 1999) Head of Human-Machine Interaction applied research Division at the Centre d'Études de la Navigation Aérienne (now DSNA/DTI/EEI). He is the author of Rejeu, the traffic simulator used for this study.

Nicolas Durand graduated from the École Polytechnique de Paris in 1990 and the École Nationale de l'Aviation Civile (ENAC) in 1992. He has been a design engineer at the Centre d'Études de la Navigation Aérienne (now DSNA/DTI R&D) since 1992, holds a Ph.D. in Computer Science (1996) and got his HDR (french equivalent of tenure) in 2004. He is currently professor at the ENAC/MAIAA (Applied Maths, Computer Science, Automatic applied to Aviation) laboratory.

Guido Manfredi graduated from Université de Sherbrooke (2011) and ENSIIE (2012) as a computer science engineer with an image processing specialization, he received his PhD in vision processing and robotics from LAAS-CNRS (2015). He is currently a researcher for the ENGIE Ineo – Groupe ADP – Safran RPAS Chair, led by ENAC. His interests include drones integration in the civil airspace, more specifically the Detect And Avoid concept and all the associated challenges.